

Supplementary material

Modeling the Mineralization Kinetics of Visible Led Graphene Oxide/Titania Photocatalytic Ozonation of an Urban Wastewater Containing Pharmaceutical Compounds

Fernando J. Beltrán *, Manuel Checa, Javier Rivas, and Juan F. García-Araya

Department of Chemical Engineering and Physical Chemistry , University Institute of Research in Water, Climate Change and Sustainability (IACYS), University of Extremadura. 06006 Badajoz, Spain; mcheca@unex.es (M.C.); fjrivas@unex.es (J.R.); jfgarcia@unex.es (J.F.G.-A.)

* Correspondence: fbeltran@unex.es; Tel.: 34-924-289387

1. Changes of Experimental Concentrations of Ozone Dissolved in Water and Hydrogen Peroxide with Time during the Second Reaction Period of Ozonation and Photocatalytic Ozonation

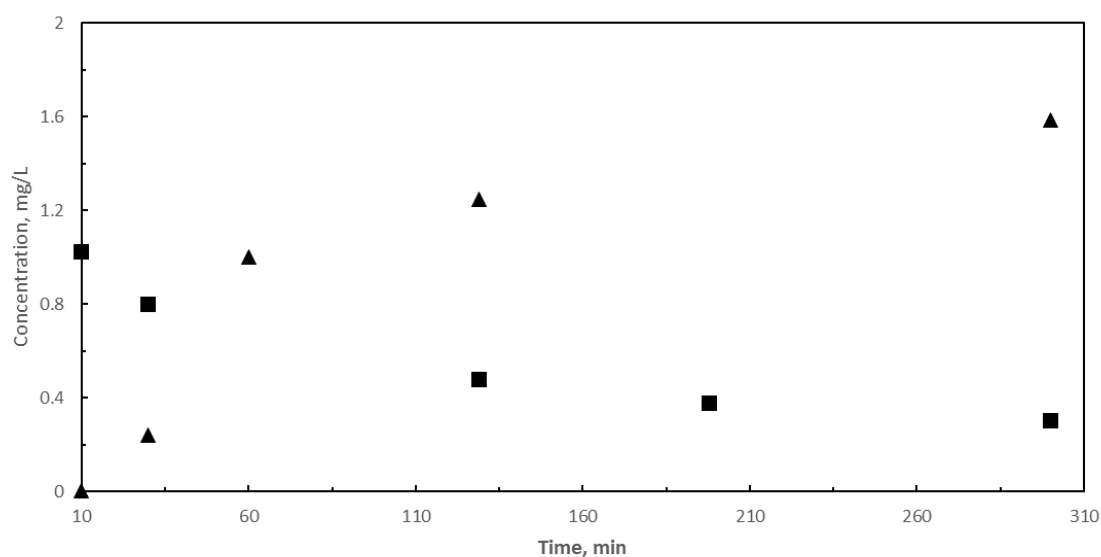


Figure S1. Single ozonation: Changes with time of concentrations of dissolved ozone (▲) and hydrogen peroxide (■) during the second reaction period. Experimental conditions as in Figure 1.

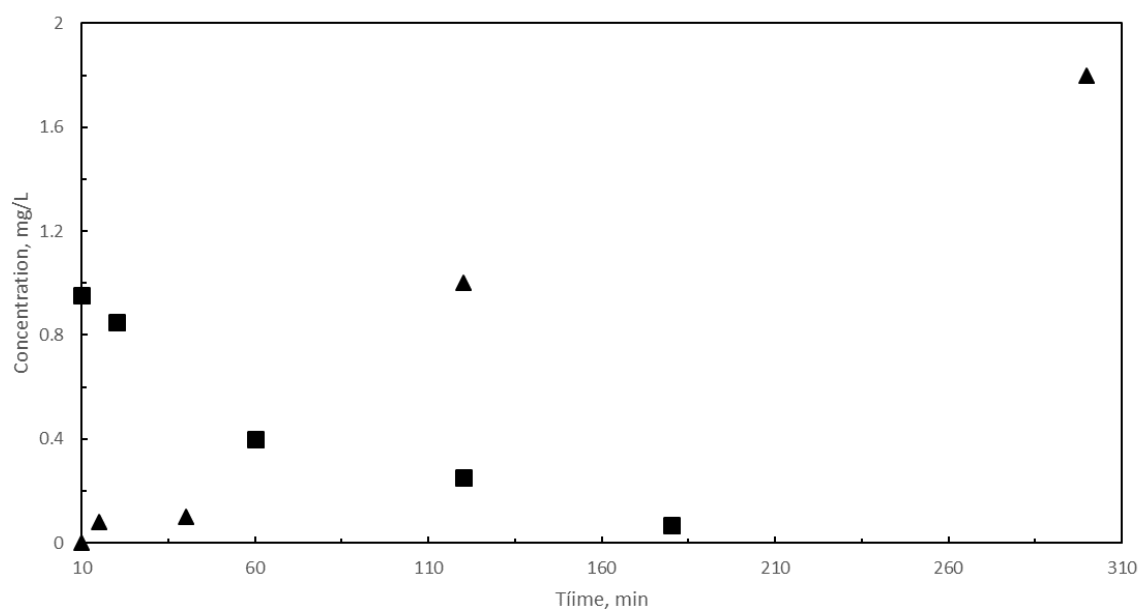


Figure S2. Photocatalytic ozonation: Changes with time of concentrations of dissolved ozone (▲) and hydrogen peroxide (■) during the second reaction period. Experimental conditions as in Figure 2.

2. Values of Some Properties and Constants to Solve the Kinetic Models

Ozone molar rate at the reactor inlet: $m_{O_3e} = 2.02 \times 10^{-6} \text{ mol s}^{-1}$

Gas flow rate: $v_g = 9.7 \times 10^{-3} \text{ L s}^{-1}$

pH = 7.5

Henry constant for the ozone-wastewater system, H_e : 109.65 atm L mol⁻¹

Volumetric mass transfer coefficient, k_{La} : $1.33 \times 10^{-2} \text{ s}^{-1}$

Individual mass transfer coefficient, k_L : $2.83 \times 10^{-5} \text{ m s}^{-1}$

Ozone diffusivity in wastewater, D_{O_3} : $1.3 \times 10^{-9} \text{ m}^2 \text{ s}^{-1}$
 TOC diffusivity in wastewater, D_{TOC} : $6.31 \times 10^{-10} \text{ m}^2 \text{ s}^{-1}$
 Liquid hold-up, β : 0.95
 Reaction volume, V : 0.5 L

3. Procedure to Determine the k_D Function of Time for the First Reaction Period

This section shows how a relationship between k_D and time was obtained for the first reaction period. The procedure was as follow: First, experimental TOC results due to pharmaceuticals were fitted to decreasing exponential functions of time (with R^2 higher than 0.99). Then, at each reaction time where experimental TOC data was available, the reaction factor F was calculated from the ratio between the experimental TOC removal rate, once the stoichiometry of reaction (1) was accounted for, and the maximum physical absorption rate of ozone as follows:

$$F = \frac{-z \frac{d\text{TOC}}{dt}}{k_L a \frac{C_{O_3g} RT}{H_e}} \quad (\text{S1})$$

Notice that the numerator of the right side of equation (S1) is the actual ozone absorption rate. Then, F_i the instantaneous reaction factor was calculated for the same reaction time with equation (7) and the corresponding Ha number with equation (6) by trial and error with known values of F and F_i . Finally, equation (8) was used to obtain the value of k_D for the reaction time considered. This procedure was repeated for successive reaction times until a value of Ha lower than 1 was obtained which meant the end of first reaction period due to fast gas liquid reactions. For single and photocatalytic ozonations, the corresponding times were 8 and 7 min, respectively. The last step was to fit k_D values to another decreasing exponential function with time that was later used to solve the kinetic model for this reaction period as indicated in section 3.1. These exponential equations for the experiments shown in Figures 1 and 2 were:

For single ozonation, valid for the first 8 min of reaction:

$$k_D = 10^6 \exp(-0.016t), \text{M}^{-1} \text{s}^{-1} \quad \text{with } R^2 = 0.97 \quad (\text{S2})$$

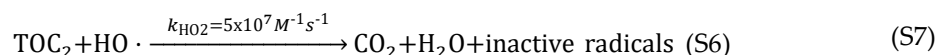
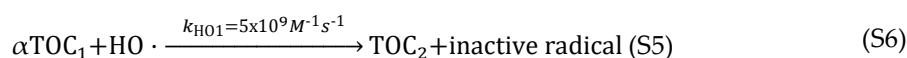
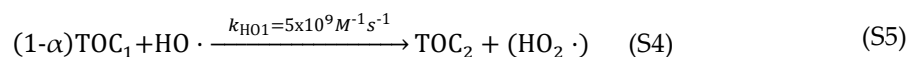
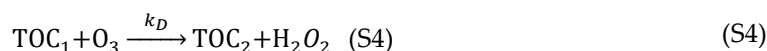
For photocatalytic ozonation, valid for the first 7 min of reaction:

$$k_D = 2 \times 10^6 \exp(-0.018t), \text{M}^{-1} \text{s}^{-1} \quad \text{with } R^2 = 0.98 \quad (\text{S3})$$

4. Mechanism of Reactions Proposed for the Second Reaction Period

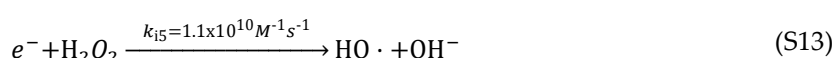
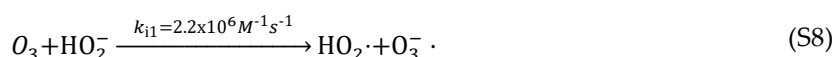
According to literature, when the kinetic regime of ozone absorption is slow both direct and hydroxyl radical reactions can compete for the organics in water [1]. Therefore, the mechanism of reactions proposed for the kinetic model of the second reaction period is constituted by ozone direct, free radical and photocatalytic reactions, depending on the ozonation process [2–6].

Reactions of TOC_1 and TOC_2 : TOC_1 was assumed to react both directly with ozone and with hydroxyl radicals by competing reactions. In these reactions TOC_2 is formed. Since TOC_1 is partially constituted by remaining pharmaceuticals and first intermediates of similar reactivity, it was assumed the formation of hydrogen peroxide due to breaking of aromatic ring and carbon double bonds [7, 8]. TOC_2 should be constituted by non reacting compounds with ozone so that it will only react with hydroxyl free radicals. Also, TOC_2 is assumed to be scavenger of hydroxyl radicals, that is, these reactions do not propagate the formation of active radicals. Something similar has been assumed for TOC_1 but in this case, only a fraction α of this TOC is considered scavenger as happens with many other ozone reacting compounds [3]. The rest of TOC_1 was considered as promoter of ozone decomposition since the hydroperoxide radical, HO_2 , is assumed to be formed [3]. Then, there are two reactions of TOC_1 with hydroxyl radicals as shown below (see reactions (S5) and (S6)). Values of the rate constant of free radical reactions with TOC_1 and TOC_2 were taken as 5×10^9 and $5 \times 10^7 \text{ M}^{-1} \text{s}^{-1}$, respectively [2]:

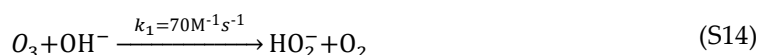


In no case, direct photolysis of TOC_1 and TOC_2 was included since pharmaceuticals and the organics present in the wastewater do not absorb radiation emitted by LEDs used ($\lambda = 425 \text{ nm}$). This also applies to ozone and hydrogen peroxide for the same reason.

Initiation reactions: These come from catalyst radiation absorption that generates charge carriers (holes and electrons) and reactions of ozone with hydrogen peroxide ionic form and with electrons from the catalyst conduction band. Electrons also react with oxygen and hydrogen peroxide to yield more initiation reactions. The stoichiometry of these reactions and corresponding reaction rate constants are [2–6]:



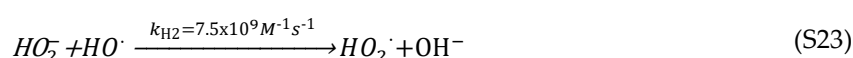
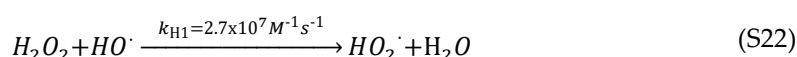
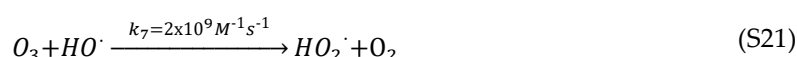
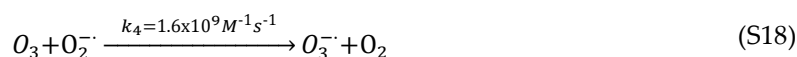
Other starting reactions are:



Charge carrier recombination:

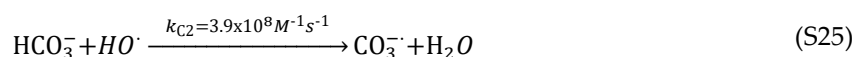
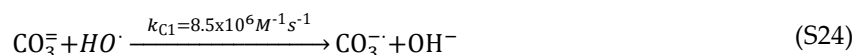


Propagation reactions:

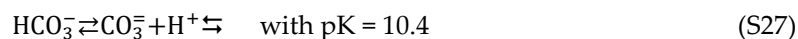
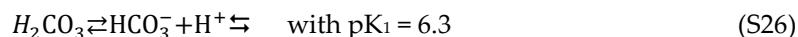


Termination reactions:

Here, recombination reactions between free radicals have been neglected because of the presence of hydroxyl radical scavengers in the treated wastewater, specifically, carbonates, TOC_2 and fraction α of TOC_1 . Scavenger reactions for carbonates are [6]:



With corresponding equilibria:



Also, termination reactions are reactions (S6) and (S7).

Mass transfer step: Another fundamental step is the ozone mass transfer to water:



5. Rate Equations, R_i , for Charge Carriers and Free Radical Species

From the mechanism, rate equations for R_i of all participating species can be obtained. For main molecular species, rate equations are in section 3.2, for charge carriers and free radicals, R_i is as follows:

For holes and electrons:

$$R_{h^+} = r_{\text{vis}} - C_{h^+} (k_{i2} + k_r C_{e^-}) \quad (\text{S29})$$

$$R_{e^-} = r_{\text{vis}} - C_{e^-} (k_{i3} C_{\text{O}_2} + k_{i4} C_{\text{O}_3} + k_{i5} C_{\text{H}_2\text{O}_2\text{T}} + k_r C_{e^-}) \quad (\text{S30})$$

where r_{vis} is the mean rate of effective photon absorption by catalyst (see section 3.2.1).

For free radicals:

Superoxide ion radical, $\text{O}_2^{\cdot-}$:

$$R_{\text{O}_2^{\cdot-}} = k_{i1} C_{\text{H}_2\text{O}_2} C_{\text{O}_3} + k_{i3} C_{e^-} C_{\text{O}_2} + (k_7 C_{\text{O}_3} + k_H C_{\text{H}_2\text{O}_2\text{T}} + (1-\alpha) k_{\text{H}_2\text{O}_1} \text{TOC}_1) C_{\text{H}_2\text{O}_2} - k_4 C_{\text{O}_3} C_{\text{O}_2^{\cdot-}} \quad (\text{S31})$$

Ozonized ion radical, $\text{O}_3^{\cdot-}$:

$$R_{\text{O}_3^{\cdot-}} = k_{i1} C_{\text{H}_2\text{O}_2} C_{\text{O}_3} + k_{i4} C_{e^-} C_{\text{O}_3} + k_4 C_{\text{O}_3} C_{\text{O}_2^{\cdot-}} - 10^{-\text{pH}} k_5 C_{\text{O}_3^{\cdot-}} \quad (\text{S32})$$

Hydrogen trioxxygen radical, HO_3^{\cdot} :

$$R_{\text{HO}_3^{\cdot}} = 10^{-\text{pH}} k_5 C_{\text{O}_3^{\cdot-}} - k_6 C_{\text{HO}_3^{\cdot}} \quad (\text{S33})$$

Hydroxyl radical, $\text{HO} \cdot$:

$$R_{\text{HO} \cdot} = k_{i2} C_{h^+} + k_6 C_{\text{HO}_3^{\cdot}} + k_{i5} C_{e^-} C_{\text{H}_2\text{O}_2\text{T}} + (k_7 C_{\text{O}_3} + k_H C_{\text{H}_2\text{O}_2\text{T}} + k_{\text{H}_2\text{O}_1} \text{TOC}_1 + k_{\text{H}_2\text{O}_2} \text{TOC}_2 + k_{\text{sc}} C_{\text{sc}}) C_{\text{HO} \cdot} \quad (\text{S34})$$

Note that there is no need to use the reaction rate of the hydroperoxide radical, HO_2^{\cdot} , since at pH 7.5 (mean pH of the wastewater secondary effluent during ozonation processes that decreased from 8 to 7) reaction (S17) is totally shifted to the right side. Then, any HO_2^{\cdot} formed immediately becomes one $\text{O}_2^{\cdot-}$.

In equations (S29) and (S30), charge carrier recombination rate ($k_r C_e C_{h^+}$) was considered negligible given the presence of GO on the catalyst and also the action of ozone, hydrogen peroxide and oxygen to capture electrons (reactions (S11) to (S13)). Therefore, reaction rate of holes, $k_{i2} C_{h^+}$, in equation (S29) was considered equal to the effective mean rate of photon absorption, r_{vis} , given by equation (21) of main text.

6. Equations for Charge Carriers and Some Important Free Radicals

From application of the steady state situation to mass balances of charge carriers and free radicals (equations (9) in main text), once reaction rates, R_i , have been substituted, the following equations were obtained for the concentrations of these species present in mass balances of molecular species (equations (13) to (15) and (18) of main text):

For concentration of electrons:

$$C_{e^-} = \frac{r_{Vis}}{k_{13}C_{O_2} + k_{14}C_{O_3} + k_{15}C_{H_2O_2T}} \quad (S35)$$

For concentration of superoxide ion radicals:

$$C_{O_2^-} = \frac{k_{11}C_{H_2O_2} \cdot C_{O_3} + k_{13}C_{e^-} \cdot C_{O_2} + (k_7C_{O_3} + k_H C_{H_2O_2T} + (1-\alpha)k_{H_2O_1}TOC_1)C_{H_2O}}{k_4C_{O_3}} \quad (S36)$$

For concentration of hydroxyl radicals:

$$C_{HO^\cdot} = \frac{2r_{Vis} + 2k_{11}C_{H_2O_2} \cdot C_{O_3}}{\alpha k_{H_2O_1}TOC_1 + k_{H_2O_2}TOC_2 + k_{sc}C_{sc}} \quad (S37)$$

7. Starting Values of Parameters to Solve the Kinetic Models

For the first reaction period:

Ozonation: At $t = 1$ min (start of the kinetic model):

TOC (of pharmaceuticals) = 2.85×10^{-3} M (34.2 mg L⁻¹), $C_{O_3g} = 3.22 \times 10^{-5}$ M (1.55 mg L⁻¹)

Photocatalytic ozonation: At $t = 1$ min (start of the kinetic model):

TOC (of pharmaceuticals) = 2.94×10^{-3} M (35.3 mg L⁻¹), $C_{O_3g} = 3.45 \times 10^{-5}$ M (1.66 mg L⁻¹)

For the second reaction period:

Ozonation: At $t = 10$ min (start of the kinetic model)

$TOC_1 = TOC$ (total) = 4.24×10^{-3} M (50.9 mg L⁻¹); $TOC_2 = 0$; $C_{O_3g} = 1.75 \times 10^{-4}$ M (8.4 mg L⁻¹); $C_{O_3} = 0$; $C_{H_2O_2T} = 3 \times 10^{-5}$ M (1.02 mg L⁻¹) (likely organic peroxides also included).

Photocatalytic ozonation: At $t = 10$ min (start of the kinetic model)

$TOC_1 = TOC$ (total) = 3.94×10^{-3} M (47.3 mg L⁻¹); $TOC_2 = 0$; $C_{O_3g} = 1.79 \times 10^{-4}$ M (8.6 mg L⁻¹); $C_{O_3} = 0$; $C_{H_2O_2T} = 2.8 \times 10^{-5}$ M (0.95 mg L⁻¹) (likely organic peroxides also included).

8. Changes with Time of Calculated and Experimental Concentrations of Ozone Dissolved in Water and Hydrogen Peroxide during the Second Reaction Period of Ozonation

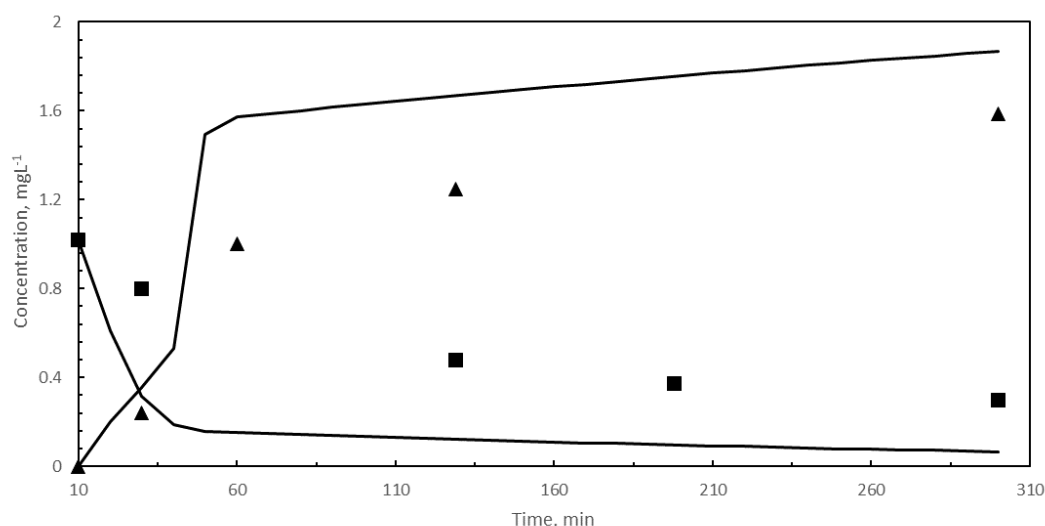


Figure S3. Kinetic model results in ozonation. Second reaction period. Changes with time of calculated and experimental concentrations of dissolved ozone and hydrogen peroxide. Black symbols: experimental results. Curves: calculated results: ■ Hydrogen peroxide, ▲ O_3 . Note that experimental hydrogen peroxide concentrations likely include the one of organic peroxides. Experimental conditions as in Figure 1.

9. Calculated Time Concentration Profiles for Hydroxyl Radicals

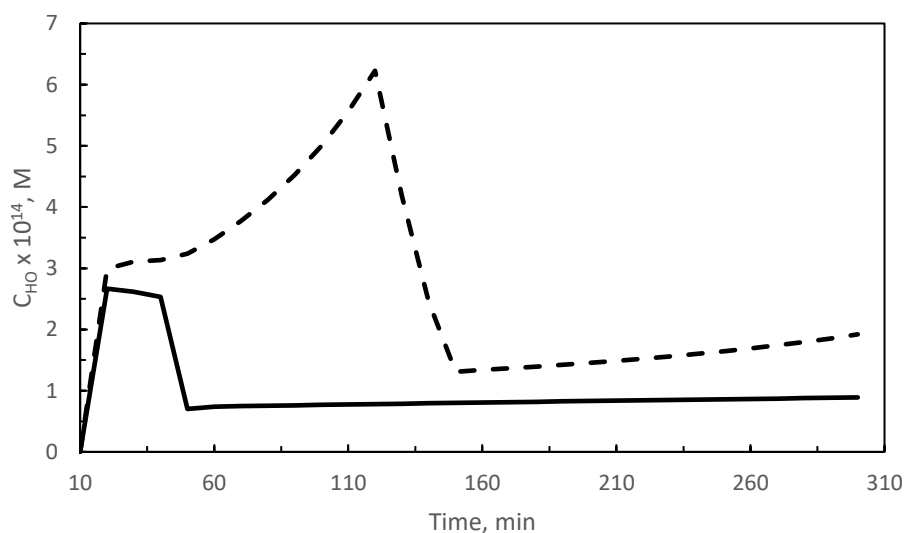


Figure S4. Kinetic model results for the second reaction period. Changes with time of calculated concentrations of hydroxyl radicals. In ozonation: Continuous line, In photocatalytic ozonation: dotted line.

10. Changes of Calculated and Experimental Concentrations of Ozone Dissolved in Water and Hydrogen Peroxide with Time during the Second Reaction Period of Photocatalytic Ozonation

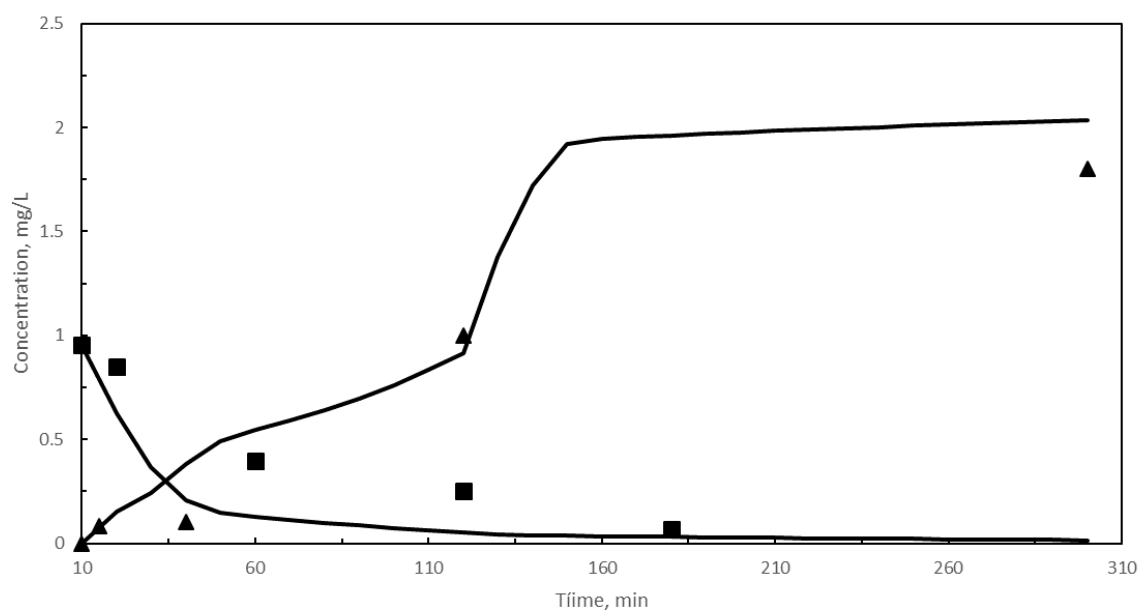


Figure S5. Kinetic model results in photocatalytic ozonation. Second reaction period. Changes with time of calculated and experimental concentrations of dissolved ozone and hydrogen peroxide. Black symbols: experimental results. Curves: calculated results: ■ Hydrogen peroxide, ▲ Co_3 . Note that experimental hydrogen peroxide concentrations likely include the one of organic peroxides. Experimental conditions as in Figure 2.

11. ANOVA Results

An ANOVA analysis of the experimental and predicted data from the model shows its viability for single and PhCatOz processes as seen in Tables S1 and S2 for first and second reaction periods,

respectively. The analysis was performed with the ANOVA statistic tool of OriginPro 2018® software, establishing a significance level of 0.05. Similar tendencies in the prediction model can be found in both ozonation and photocatalytic process. Also, Figures S6 and S7 for the first reaction period and Figures S8 and S9 for the second reaction period show experimental versus predicted TOC and ozone gas concentration at the reactor outlet results. It is seen that deviations of calculated data are within $\pm 10\%$ of experimental results.

Table S1. ANOVA statistics of the kinetic model at 0.05 significance level for the first reaction period.

	Parameter	R ²	Coeff Var	Root MSE
Ozonation	TOC	0,99252	0,06454	1,15252
	CO _{3gas}	0,9795	0,08659	0,45198
PhCatOz	TOC	0,99133	0,07903	1,31539
	CO _{3gas}	0,99589	0,04928	0,2282

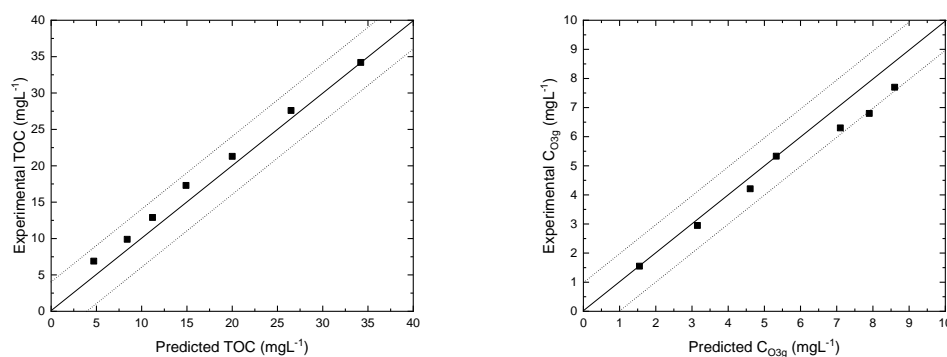


Figure S6. Experimental vs predicted values of TOC and CO_{3g} in Ozonation for the first reaction period. Dotted lines correspond to $\pm 10\%$ deviations.

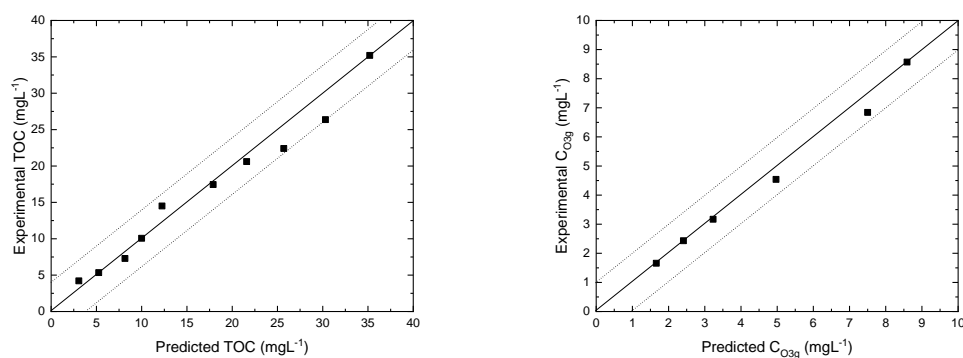
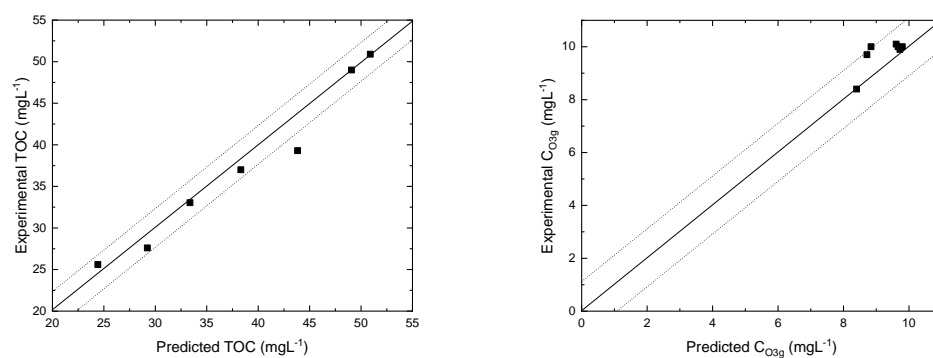
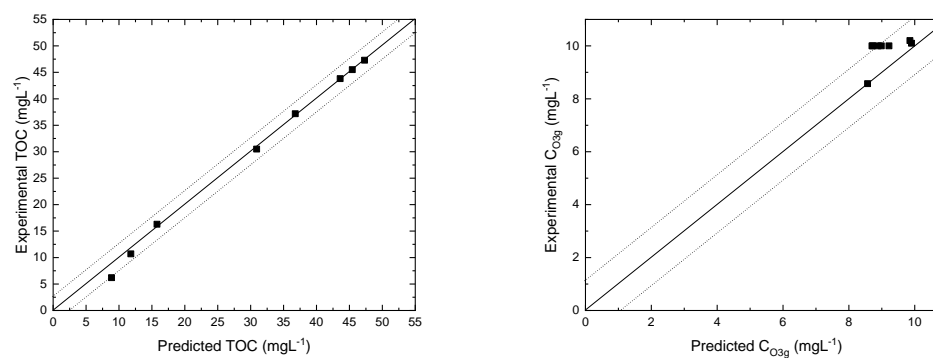


Figure S7. Experimental vs predicted values of TOC and CO_{3g} in PhCatOz for the first reaction period. Dotted lines correspond to $\pm 10\%$ deviations.

Table S2. ANOVA statistics of the kinetic model at 0.05 significance level for the second reaction period.

	Plot	R ²	Coeff Var	Root MSE
Ozonation	TOC	0,9888	0,03624	1,37595
	CO _{3gas}	0,72414	0,04657	0,44196
	CO ₃	0,94468	0,1827	0,21203
	CH ₂ O ₂	0,79507	0,48293	0,22157
PhCatOz	TOC	0,99877	0,02509	0,74954
	CO _{3gas}	0,47667	0,0665	0,63055
	CO ₃	0,97959	0,17872	0,14601
	CH ₂ O ₂	0,93424	0,30507	0,13105

**Figure S8.** Experimental vs predicted values of TOC and CO_{3g} in Ozonation for the second reaction period. Dotted lines correspond to $\pm 10\%$ deviations.**Figure S9.** Experimental vs predicted values of TOC and CO_{3g} in PhCatOz for the second reaction period. Dotted lines correspond to $\pm 10\%$ deviations.

12. XRD Analysis of GO/TiO₂ Catalyst

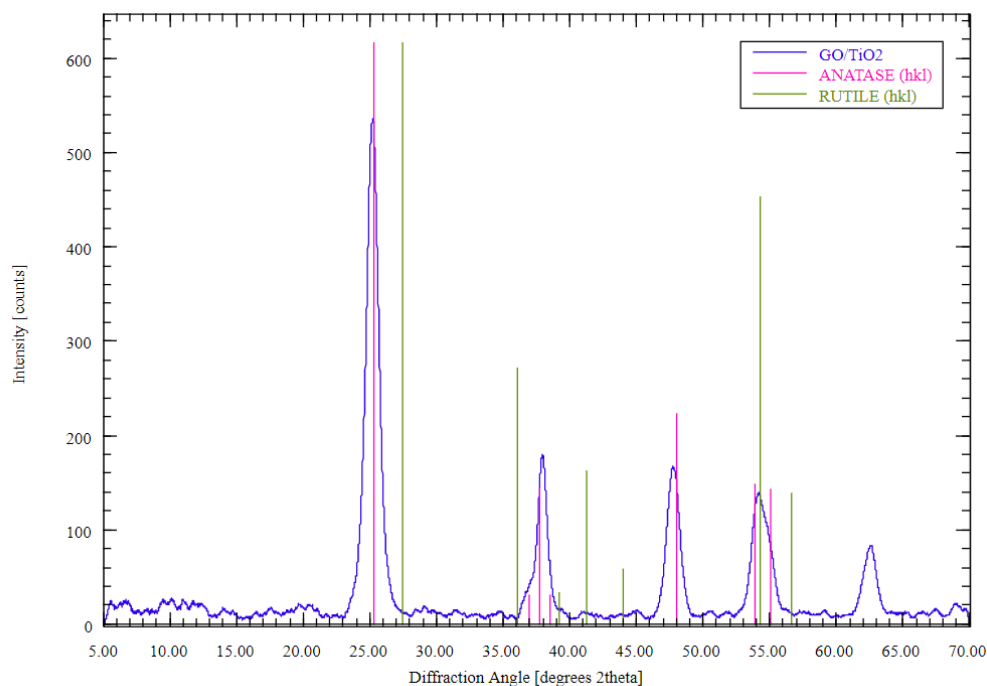


Figure S10. XRD of GO/TiO₂ composite.

References

1. Beltrán, F.J., *Ozone reaction kinetics for water and wastewater systems* Lewis Publishers: Florida, U.S., **2004**; pp. 1-358
2. Buxton, G.V.; Greenstock, C.L.; Helman, W.P.; Ross, A.B. Critical review of data constants for reactions of hydrated electrons, hydrogen atoms and hydroxyl radicals (OH/O[•]) in aqueous solution. *J. Phys. Chem. Ref. Data*, **1988**, *17*, 513–886
3. Staehelin, S.; Hoigné, J. Decomposition of Ozone in Water the Presence of Organic Solutes Acting as Promoters and Inhibitors of Radical Chain Reactions. *Environ. Sci. Technol.*, **1985**, *19*, 1206 - 1212.
4. Staehelin, S.; Hoigné, J. Decomposition of ozone in water: Rate of initiation by hydroxyde ions and hydrogen peroxide, *Environ. Sci. Technol.*, **1982**, *16*, 666–681.
5. Christensen, H.S.; Sehested, H.; Corfitzan, H. Reactions of hydroxyl radicals with hydrogen peroxide at ambient and elevated temperatures. *J. Phys. Chem.*, **1982**, *86*, 55–68.
6. Weeks, J.L.; Rabani, J. The pulse radiolysis of deaerated carbonate solutions. 1. Transient optical spectrum and mechanism. 2. pK for OH radicals. *J. Phys. Chem.*, **1966**, *82*, 138–141.
7. Mvula, E.; von Sonntag, C. Ozonolysis of phenols in aqueous solution, *Org.Biomol.Chem.* **2003**, *1*, 1749–1756.
8. Leitzke, A.; von Sonntag, C. Ozonolysis of unsaturated acids in aqueous solution: acrylic, methacrylic, maleic, fumaric and muconic acids. *Ozone Sci.Eng.* **2009**, *31*, 301–308.



© 2020 by the authors. Submitted for possible open access publication under the terms and conditions of the Creative Commons Attribution (CC BY) license (<http://creativecommons.org/licenses/by/4.0/>).